

# Short Papers

## Self-Aligning Exoskeleton Axes Through Decoupling of Joint Rotations and Translations

Arno H. A. Stienen, Edsko E. G. Hekman, Frans C. T. van der Helm, and Herman van der Kooij

**Abstract**—To automatically align exoskeleton axes to human anatomical axes, we propose to decouple the joint rotations from the joint translations. Decoupling can reduce setup times and painful misalignment forces, at the cost of increased mechanical complexity and movement inertia. The decoupling approach was applied to the Dampace and Limpact exoskeletons.

**Index Terms**—Exoskeleton, kinematics, mechanism design, physical human-robot interaction, rehabilitation robotics, upper limb.

### I. INTRODUCTION

Patient-friendly robots are used as diagnostic and therapeutic aids in upper extremity rehabilitation. Through physical manipulation of the arm and assisted by virtual environments, innovative interaction schemes are explored in search of the best possible therapy. Overall, robot-assisted therapy is considered to be as good or better than conventional therapy [1]–[4]. It is more challenging for the patients and less labor intensive for the therapists and has provided the physicians, therapists, and scientific community with more reliable data.

Robot rehabilitation devices for the upper extremities can be grouped into endpoint manipulators [5], [6], exoskeletons [7]–[12], and cable suspensions [13], [14]. Of these, exoskeletons are well-suited for direct manipulation and measuring of the joint angles and torques. The external skeleton runs parallel to the upper and lower arm and has actuators and sensors directly on the joints. Unfortunately, for typical exoskeletons to function correctly their axes need to be closely aligned to the anatomical axes of the human joints. Without correct alignment, the exoskeleton will feel uncomfortable in use [15], up to the point of becoming unusable. Alignment can take as much as 5–15 min, cutting into the valuable rehabilitation time available for each patient.

Three reasons make alignment difficult to attain. First of all, human joints are seldom simple hinges. The shoulder girdle, for example, has not only three rotational degrees of freedom (DOFs), but also two translational ones due to the rotation of the clavicle with respect to the thorax [16]–[18]. Humans have some voluntary control over shoulder translations, but the vertical translation is also coupled with the shoulder elevation rotation [19] and is known as the scapulohumeral

Manuscript received February 20, 2009; revised March 16, 2009. First published April 17, 2009; current version published June 5, 2009. This paper was recommended for publication by Associate Editor M. Johnson and Editor K. Lynch upon evaluation of the reviewers' comments. This work was supported by SenterNovem (NL) under Grant TSGE2050.

A. H. A. Stienen is with the Laboratory for Biomechanical Engineering, University of Twente, 7500 AE Enschede, The Netherlands. He is also with the Physical Therapy and Human Movement Sciences, Northwestern University, Chicago, IL 60611 USA (e-mail: arnostienen@gmail.com).

E. E. G. Hekman is with the Laboratory for Biomechanical Engineering, University of Twente, 7500 AE Enschede, The Netherlands (e-mail: hekman@utwente.nl).

F. C. T. van der Helm and H. van der Kooij are with the Laboratory for Biomechanical Engineering, University of Twente, 7500 AE Enschede, The Netherlands, and also with the Laboratory for Biomechanical Engineering, Delft University of Technology, 2628 CD Delft, The Netherlands (e-mail: f.c.t.vanderhelm@tudelft.nl; h.vanderkooij@utwente.nl).

Digital Object Identifier 10.1109/TRO.2009.2019147

rhythm. Second, the exact location of the human axes cannot be seen from the outside without the help of imaging devices. Bony landmarks only give a general approximation of the location of the rotation axes, with significant differences between people. Finally, the positioning of the exoskeleton on the arm may differ between therapy sessions, thus always requiring final adjustments, even if device settings are stored for later recollection. However, even when close alignment is achieved before therapy is started, the cuffs may slip during usage, requiring further adjustments [20].

Current exoskeletons solve the joint alignment and shoulder translation problems in different ways. The CADEN-7 [12] and the L-EXOS [9] use no additional mechanisms but do not fix the trunk and, thereby, force the body to make any necessary translations relative to the exoskeleton shoulder position. The different variations of WREX exoskeletons [8], [21] have additional two-link mechanisms for horizontal shoulder translations with two DOFs. The ARMin [10] uses a vertical four-link mechanism that couples the shoulder elevation rotation of the exoskeleton to its vertical shoulder translation with a single DOF. Finally, the MGA exoskeleton [11] adds a rotational DOF to the shoulder, mimicking clavicle rotations to produce the vertical translations for the exoskeleton shoulder.

For all of the aforementioned exoskeletons, the elbow and shoulder joints need to be aligned as closely as possible to minimize any possible problems. By adding a large number of passive links to the actuated ones, the exoskeleton of the European Space Agency [15] requires no joint alignment. However, its actuators and linear-motion joints are optimized for low-force haptic interaction to control space robots and are underpowered and unsuitable for many rehabilitation exercises.

The goal of this paper is to determine the suitability of decoupling joint rotations and translations for use in upper extremity rehabilitation robots. As we will make clear, decoupled joints theoretically align themselves to the human anatomy. They are an alternative to conventional joint designs and may overcome many of the problems traditionally associated with exoskeletons. This paper describes the decoupling for the shoulder and elbow joints, the mechanical requirements, the advantages and disadvantages, and two implementation examples.

### II. ANALYSIS

#### A. Decoupling of Rotations and Translations

Most exoskeletons are firmly connected to the global world. When their axes are misaligned, any rotation forces relative translations on the human joint [see Fig. 1(a)]. This translation is forced on the skin, the internal musculoskeletal system, and the trunk. Of these, the musculoskeletal system may not be able to translate in a required direction, and the trunk can be practically unmovable when fixed to a chair or having a large movement inertia. In such a situation, the forced translation will result in large depressions of the soft tissue between the exoskeleton and the human skeleton. Depending on the amount of misalignment, the tissue depression can be from annoying to painfully limiting, especially for patients with skin-sensitivity problems. To prevent this situation from occurring, the axes need to be perfectly aligned.

Having joint axes in both the exoskeleton and the human arm creates a redundant system, which causes the aforementioned problems. Removing the exoskeleton joints completely and mounting each exoskeleton segment directly on each arm segment removes the redundant joint axes but makes exact control of the joint angle difficult. Mechanically

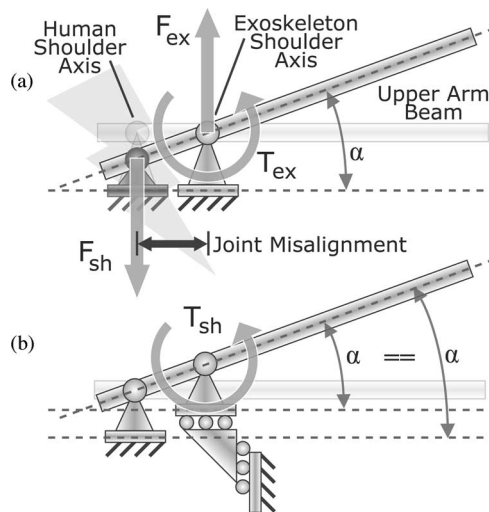


Fig. 1. Self-alignment for exoskeletons axes in a planer view. (a) The effects of a single misaligned axis at the shoulder. Due to exoskeleton torque  $T_{ex}$ , the arm and exoskeleton axes rotate an angle  $\alpha$ . If these axes are misaligned, the human joint has to translate relative to the exoskeleton axis. If the axes are fixed, this movement creates a residual shoulder force  $F_{sh}$ , which is dependent on the stiffness of skin and bone, and an equal exoskeleton reaction force  $F_{ex}$ . (b) Translating exoskeleton axes prevents these misalignment forces. If a misalignment causes a force  $F_{ex}$ , the exoskeleton translates until this force is gone. Torques can be applied to the limb from the rotational-stiff linkage mechanism. The effects are the same in 3-D by adding the two other rotational axes requiring only the one final linear axis.

decoupling the joint rotations from the joint translations may be the solution. Free translation of the exoskeleton axes—but fully constrained by the kinematics of a connected human arm—creates self-aligning axes. The decoupling allows the rotation of these axes to be controlled without affecting the self-alignment.

By mounting the exoskeleton on a movable linkage system that maintains an endpoint orientation parallel to the global world, the translations and rotations in the exoskeleton joints are decoupled [see Fig. 1(b)]. The linkage system can freely translate in any direction, solving joint misalignments instead of requiring the human body to do so; whenever a misalignment generates a reaction force, the linkage will move until a new zero-force position is reached. The endpoint connector of the linkage needs to always maintain its original orientation and should have sufficient torsional stiffness to let the exoskeleton generate torques from it onto the human arm.

The decoupling of translations and rotations influences the force interactions between the exoskeleton and human limb. Conventional exoskeletons often apply a single force to the end of a limb segment, which rotates the segment around the human axis. This also generates a reaction force at the human joint, which the musculoskeletal system of the trunk needs to counteract. With the decoupled mechanism, applying single forces to the limb becomes impossible, as the accompanying reaction force would simply translate the linkage. Instead, the forces must be applied pairwise as torques. The forces felt by the arm from the external mechanisms now consist of the impedance forces due to friction and inertia of the linkage and exoskeleton. These reaction forces are generally much lower than the aforementioned misalignment forces and the reaction forces caused by the single-force interaction, especially for low-speed movements. The local forces caused by muscle activation around each joint are, of course, still present.

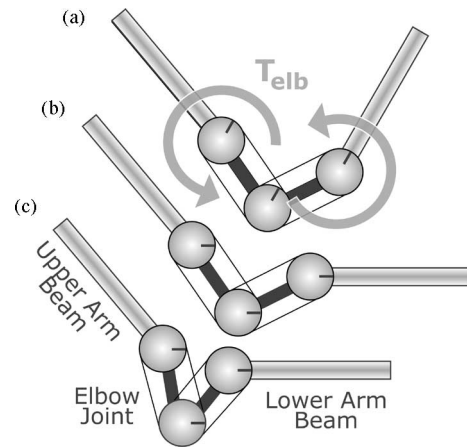


Fig. 2. Implementation of the self-alignment of Fig. 1(b) for the elbow joint. The elbow joint has two extra links, and two parallelograms transfer the forearm orientation to the upper arm. Translation of the joint is now independent of rotation (from c to b), and *vice versa* (b to a), removing the requirement for close elbow alignment. At the upper arm, the rotation can be controlled and measured; a torque applied here runs through the parallelogram and is applied to the forearm, without causing reaction forces in the elbow. The parallelogram can be created with cables and drums (as shown here) or with a push-pull design with rods.

The pairwise forces do require two connections of the exoskeleton to the limb per section. This additional cuff per section is a disadvantage, especially when it needs to be located over a thick layer of soft skin and muscle tissue. This can significantly reduce the interaction stiffness between exoskeleton and arm. Conventional exoskeletons often grip the arm at the bony parts of the elbow and wrist and not at the soft tissue just distal from the elbow and shoulder, as required for two cuffs per segment.

An advantage of the pure-torque-driven actuation is that it has now become independent of any positional misalignment, body-supplied reaction forces, or torques applied to other joints. Also, for perpendicular limb orientations, torques applied around one joint will not cause the the exoskeleton to slide over the arm. For instance, when torques are applied to the elbow, the shoulder feels no forces other than due to inertia and friction, making selective training of muscles possible. Furthermore, any torques can be directly measured without interference from other joints. However, when endpoint forces are needed, the applied torques are less realistic than applied forces by conventional exoskeletons. Although those are also less realistic than endpoint forces generated with endpoint manipulators.

The decoupling at the human shoulder requires a full 3-D linkage and three rotational DOFs. The elbow can make do with a 2-D linkage and a single rotation DOF (see Fig. 2), as the elbow axis of rotation has only a few degrees of orientation variability [22], [23]. It is important to realize that without a mounted human arm, the two additional, passive segments create an underdetermined system. However, with the decoupled joint mounted on a human arm, the passive segments are fully constrained by the kinematics of the human joint. This also applies to the additional linkage mechanics at the shoulder.

### B. Comparison of Linkages

The design of the linkage influences the experience of the subject. As described in the previous section, the impedance forces felt are due to friction and inertia in the linkage and exoskeleton. Therefore, three linkage designs were compared on their range of motion, stiffness, and impedance forces hindering movement. The three designs are the

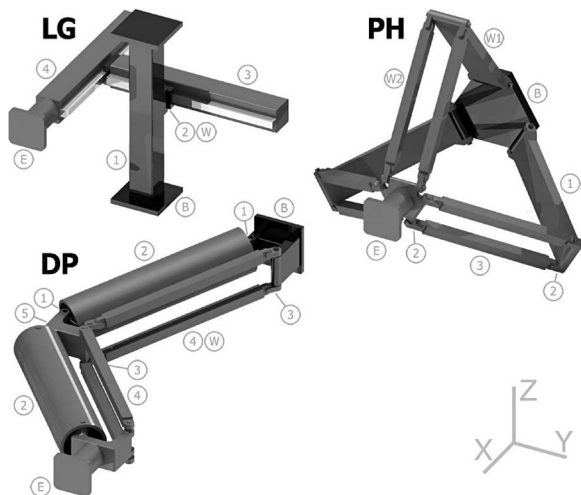


Fig. 3. Three linkages which can translate freely in 3-D space but are rotational-stiff around any axis. From left to right: Linear guidance (LG) mechanism, based on linear-motion slider rails, a parallel hexapod (PH) similar to the Delta Robot [24], [25], and a double parallelepiped (DP), which is our own design. The exoskeleton would be mounted to the front plate and the black base plate to the global reference frame.

linear guidance (LG) mechanism, the parallel hexapod (PH) similar to the Delta robot [24], [25], and the double parallelepiped (DP) as by our own design (see Fig. 3 and Table I). The LG mechanism is based on linear motion slider rails, which also have to provide the torsional stiffness. The PH get its torsional stiffness from the parallel rods connected to the base plate. In the normal workspace, almost no segment receives significant torsional load, making it possible to use very thin-walled push-pull rods. The DP uses one torsional-stiff thin-walled tube with a large diameter, and two push-pull rods per segment to handle the torsional loads around any axis. Although all linkages can be mounted with actuators, they are preferably kept passive, requiring only weight support via low inertia, ideal-spring mechanisms [14], [26].

All designs were created to have a cubic  $300 \times 300 \times 300$  mm workspace and a stiffness roughly equal to 6.5 mrad distortion when loaded with 50 Nm in a direction. The workspace is defined by the need to handle reasonable shoulder-axes misalignment of up to 10 cm [27] and some interpatient variability. This required segment lengths of respectively 350, 275, and 375 mm for the LG, PH, and the DP, respectively. A 6.5-mrad rotation equals a 7-mm translation at 1 m from the center of the linkage front plate. This arbitrarily chosen value was mostly based on the lowest stiffness of a still realistic design of the PH. The desired stiffness defined the segment strengths and the distance at which parallel members were placed from each other, with the dimensions and weights given in Table I. Using COSMOSWorks (Dassault Systemes) to do the finite-elements calculations on the models, the beam and rod dimensions were adjusted until their stiffnesses roughly matched (see top half of Fig. 4). These deflections were measured at the center of the work volume, representing the normal, ideal situation, when only small translations are necessary. The mechanisms were designed to have stiffnesses as independent from orientation as possible, and none will get into an extreme configuration to reach the edges of the required workspace. Toward the edges of the work volume, the stiffness will decrease exponentially by about 10% for all three designs (data not shown).

With the workspaces and stiffnesses closely matched, the inertial matrices were determined with Spacar [28], which is a multibody-dynamics analysis package (see Fig. 4). The linear motion slider rails

TABLE I  
DIMENSIONS AND WEIGHTS OF LINKAGES

[B]ase), [E]ndpoint, [Thick]ness. Values given per tube or pointmass.						
Part	Length [mm]	Height [mm]	Width [mm]	Thick [mm]	Weight [gr]	Material
<b>Linear Guidance (LG)</b>						
1	350	50	50	2	fixed	alu
	350	15	15	-		steel
2	pointmass				375	steel
3	350	50	50	2	1180	alu
	350	15	15	-		steel
pointmass					steel	
4	350	50	50	2	991	alu
	350	15	15	-		steel
pointmass					293	alu
Uses only linear ball bearings on smooth guiding rails.						
<b>Parallel Hexapod (PH)</b>						
1	275	60	20	1	200	alu
2	pointmass				63	alu
3	275	20	20	1	71	alu
pointmass					693	alu & steel
Tubes 3 are spaced 70 mm apart, center to center. Link 2 rotates around two perpendicular axes. Uses only rotation ball bearings.						
At the center of the workspace, bottom of [E] is 350 mm from [B].						
<b>Double Parallelepiped (DP)</b>						
pointmass					70	alu
2	375	90		1.25	494	alu
pointmass					63	alu
4	375	20	20	1.25	102	alu
pointmass					437	alu
pointmass					582	alu
Tubes closest to [B] rotate around vertical and horizontal axes, tubes closest to [E] only around horizontal. Uses only rotation ball bearings.						
Vertical axes rotate with $0^\circ$ (fully extended tubes) to $60^\circ$ , default at $30^\circ$ . (At $30^\circ$ , horizontal distance between thick and thin tubes is 87 mm.)						
Horizontal axes rotate from $-30^\circ$ to $30^\circ$ , default at $0^\circ$ (horizontal tubes). (At $0^\circ$ , vertical distance between thin tubes is 75 mm.)						

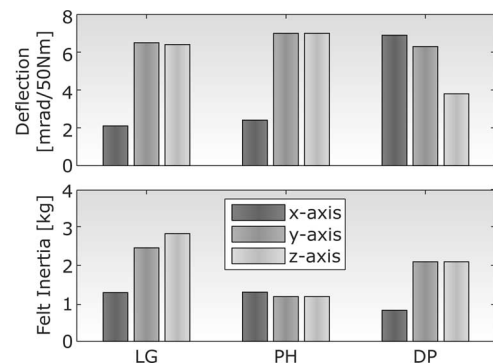


Fig. 4. Comparison of the stiffnesses and apparent inertia of the three linkages at the center of the workspace. (Top) The linkage dimensions were adjusted to have roughly equal deflection at 50 Nm of torque. The inertial matrices are displayed in the bottom figure. For LG and PH, the eigenvectors are along the XYZ-axes as indicated in Fig 3; for DP, "x-axis" indicates the eigenvector perpendicular to the lower parallelogram  $[-0.7 \ 0.7 \ 0]$  and "y-axis" the eigenvector perpendicular to the upper parallelogram  $[0.7 \ 0.7 \ 0]$ .

used in the LG system—as used in the Dampace [27]—has a load dependent friction of about 4 to 20 N. The rotational joints of the other two mechanisms have no significant friction. Coulomb friction is highly undesirable in these linkages, as it is felt at any movement speed and can be a significant force to overcome for all patients.

From these simulations, the PH has the least amount of inertia and friction, closely followed by DP. The impedance forces of the latter strongly depend on the direction of movement as it is a 2-link mechanism; for endpoint deflections perpendicular to the first stage, half the first stage and the full second stage will move, whereas for deflections perpendicular to the second, only half the second stage will move. The average inertia for all three eigenvalues of the inertia matrices stays invariant over the work volume for LG, varying up to 10% for the PH, and up to 20% for the DP, again all exponentially increasing at the edges but more or less constant in the middle (data not shown).

Three other design considerations need to be made: the possibility to add a passive weight support mechanism, the amount of space used by the segments in the linkage design, and the possibility to add actuators to the linkage. The first, i.e., passive weight support, supports the weight of the mechanism without hindering the patient. It is most difficult to add to the PH as it has multiple DOFs controlling the vertical translation, with multiple segments requiring a separate weight support mechanism (for instance, through segments  $W1$  and  $W2$  in Fig. 3, weight support system itself not shown). Both the LG system and the DP only have one vertical DOF, which is on the easily accessible first segment (segments  $W$  in Fig. 3). The second, i.e., the amount of space used, may lead to the linkage interfering with the exoskeleton or body movements. Most space is used by the PH as its three legs always point away from each other, whereas the other two use much less space. Finally, adding actuators and force sensors can further reduce the impedance by employing an admittance control loop at the cost of some system stability. This is easily added to the PH as all three actuators can be mounted on the base, working on the three single-axis segments there. Such actuation may also be used to provide active weight support but this would add a continuous electrical load to the actuators. The other two systems require either complex cabling systems or need to mount the heavy actuators directly on the segments.

Based on the ability to function as a passive mechanism (with only passive weight support added) and its slender design and low space requirements, the DP is considered best suited for the shoulder linkage system. When space requirements are less stringent or actuation desired, the PH definitely warrants further investigations.

### C. Shoulder Axes Configurations

The decoupling of translations and rotations loosens the requirements for exact axes orientation for the three shoulder rotations. As the linkage can take care of necessary exoskeleton realignments, the axes do not necessarily have to follow through the glenohumeral rotation center of the shoulder. However, any movement of the linkage will generate dynamic forces and should be reduced as much as possible. The axes orientation is also a balance between staying away from singular configurations—when two axes are inline (gimbal lock), the accelerations, and thus, inertial forces are amplified—reducing potential movement and inertia of the linkage, and obtaining the desired range of motion possible.

Positioning the third exoskeleton axis parallel to the shoulder axial rotation axis gives a misalignment of about 50 to 100 mm, depending on the thickness of the arm (see Fig. 5). This results in translations of the linkage of twice this amount for shoulder axial rotations, which is undesirable. The third exoskeleton axis can also be directed through the glenohumeral rotation center, but this requires additional changes to the

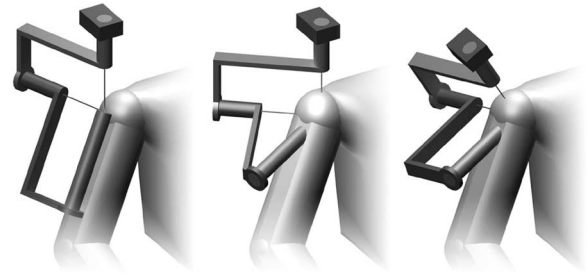


Fig. 5. Possible configurations for the shoulder axes. (Left) Due to the decoupling of the rotations and translations, the third exoskeleton shoulder axis can be positioned parallel to the shoulder axial rotation axis. This configuration, as in the Dampace [27], generates high levels of linkage movement and inertial forces. (Middle and right) To reduce these and to stay away from gimbal-lock orientations, the third exoskeleton axis can be positioned at a  $30^\circ$  angle. The axis now points to the glenohumeral rotation center. (Middle) To optimize the shoulder range of motion, either the third exoskeleton axis is not perpendicular to the second axis, or (right) the first axis is positioned at an angle to the vertical [11], [29]. Both still restrict the shoulder negative elevation rotation to  $90^\circ$  as verified with 3-D modeling software.

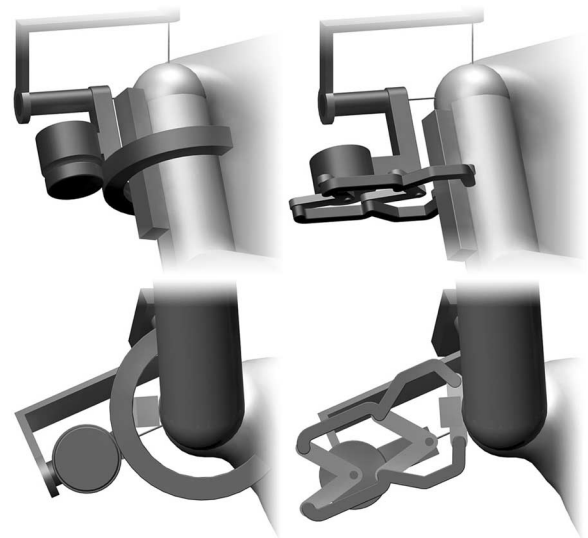


Fig. 6. Alternative third exoskeleton axis configurations. (Left) The third axis is realized with a semicircular guiding rail, powered by a motor directly attached to it. This configuration is often used in current exoskeletons [9], [10], [12] but requires high friction and heavy guiding rails. (Right) Alternatively, an external rotation center mechanism can also realize the rotation around the shoulder axial rotation axis. The mechanisms have two parallel bars and centers around the main joint connection, with one side of the bars powered by an actuator, and the other connected to off-center connections to the arm. The bottom figures are the bottom views at the mechanisms of the upper figures.

axes orientation and reduces the shoulder negative elevation rotation to about  $90^\circ$  (again, see Fig. 5).

Alternatively, the third exoskeleton axis may be aligned closer to the shoulder axial rotation axis by using additional mechanisms (see Fig. 6). Many exoskeletons [9], [10], [12] use the open, semicircular slider rail to directly align the axes, but this has several disadvantages, mainly due to the weight of the steel rail, the friction in the bend-around linear bearings, and the lack of stiffness. Using an external rotation center mechanism, based on rotational bearings, is stiffer and lighter than the semicircular guiding rail. Any

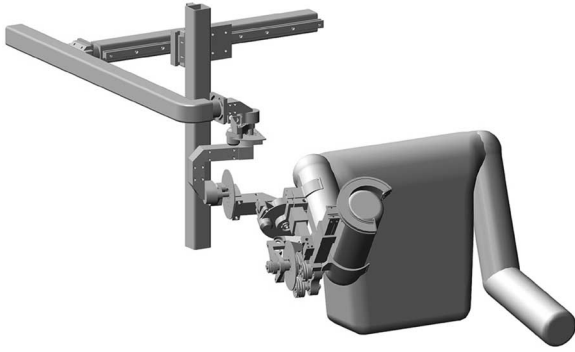


Fig. 7. Dampace exoskeleton [27], [30] has powered hydraulic disk brakes on the rotational axes of the shoulder and elbow. It uses the LG linkage system and the parallel shoulder axial rotation axes. The friction of the first and the high movement amplitudes of the second result in significant impedance during rotation of the self-aligning joints.



Fig. 8. Limpact exoskeleton [31], [32] uses rotation hydroelastic actuators on its shoulder and elbow joints. With the lessons learned from the Dampace, it uses the DP linkage mechanism and the external rotation center mechanisms at the shoulder axial rotation axis. The cabled design of the elbow joint of the Dampace has been replaced by a push-pull mechanism, which is stronger and requires less maintenance.

misalignment still present in either mechanism, for instance due to the varying thickness of the arm, will be handled by the linkage system.

#### D. Example Implementations

The information presented in this paper is based on our experiences with the Dampace [27], [30] and Limpact [31], [32] exoskeletons (see Figs. 7 and 8). The older Dampace uses the LG linkage, and its third shoulder axis runs parallel but with and offset to the upper arm. The already heavy and friction prone linkage thus has to move over large distances, especially for shoulder axial rotations. To improve on the performance, the upcoming Limpact exoskeleton uses the DP linkage and the external rotation center mechanisms for the axial rotations of the shoulder. For the elbow joint, the parallelogram cables have been replaced by push-pull mechanisms, thus requiring less maintenance.

### III. DISCUSSION

Decoupling of the joint rotations and joint translations creates self-aligning exoskeleton joints. It removes the requirement of closely aligning the exoskeleton axes to the anatomical ones during setup. Decoupling gives the responsibility of solving joint misalignment to the exoskeleton and not the human musculoskeletal system, the full body, or the soft tissue between the arm and the exoskeleton. By doing so, it prevents the interaction with the exoskeleton from becoming painful [15], [33]. Decoupling also significantly reduces setup times, which is essential for use in stroke rehabilitation. The freely translating linkage gives the shoulder full freedom of translation, making voluntary and coupled translations [19] possible, independent of the rotations of the joint. Linkage translation also assists in adjusting the setup because of interpatient differences in trunk height and width. Exoskeleton segment lengths still need to be adjusted when changing subjects. However, with decoupling, these adjustments do not need to be exact as they now have less influence on the joint alignment.

It is important to remember that when not connected to the arm, these passive linkages are free to translate in any direction. With the exoskeleton mounted to the arm, however, the translation kinematics of the linkages are fully constrained by the kinematics of the arm. In effect, decoupling removes the redundant positioning of the second axis created by conventional exoskeleton joints.

Several types of passive, weight-supported linkages can be used to decouple the rotations and translations. All of them significantly increase the device complexity and movement inertia. The three linkages in this study are all rotationally stiff, while they allow translation in any direction. The PH and DP linkages require a large number of additional machined components and bearings. This makes the device heavier, more costly, and more likely to fail. Then again, the linkages are not much more complex than the additional mechanics used for shoulder translations in the ARMin [10], the cable guiding mechanisms in the CADEN-7 [12], or the additional clavicle-limb in the MGA-Exoskeleton [11]. For reasons of minimal space usage, low impedance, and easy inclusion of weight support, the DP is our preferred linkage. With unactuated linkage mechanisms, decoupled joints also give less guidance to, for instance, the humerus head than conventional exoskeletons. With such guidance, the humerus head can be positioned such as to avoid training with a subluxated shoulder.

An exoskeleton with decoupled joints can only transfer torques, which is a possible second disadvantage. Single forces would just push the linkage away instead of being applied to the arm. Torque transfers require two connections per segment. These cannot always be located at bony parts of the arm and, therefore, reduce the overall interaction stiffness between the exoskeleton and limb. At the upper arm, one cuff can be positioned directly under the arm pit and the other just above the elbow, thus, on either side of the biceps. For the forearm, the cuffs go just distal from the elbow and at the wrist. To allow pro/supination of the forearm, the wrist cuff needs to be able to rotate, possibly with an open, semicircular guiding rail. The first three of these cuffs go on slack tissue, which is a problem for some people. For them, with torques above 20 N·m, the cuffs will press on the skin and muscles, resulting in an angle mismatch between exoskeleton and arm.

For the shoulder joint, the decoupling also solves many of the misalignment problems caused by voluntary and forced translations. Conventional exoskeletons have fewer problems with aligning their elbow joints, but even there, a self-aligning mechanism has the advantage of shorter setup times and less of a need for accurate positioning.

In this paper, the decoupling and the required linkages are described for the shoulder and elbow joint, but they could easily be adapted

for the lower extremities. For the knee joint, the 2-D self-aligning mechanisms could handle both the rotation and the coupled translation specific for this joint. For the hip joint, either several 2-D mechanisms could be stacked or one 3-D mechanism used. A disadvantage specific to the lower extremities could be the mainly vertical orientation of the segments. As each exoskeleton segment is connected to each leg segment, without strong translational couplings to other exoskeleton segments, individual cuffs may slip due to gravity and cyclical inertial forces. It would not necessarily influence the self-alignment, but the cuff movement may irritate subjects.

In conclusion, decoupling of joint rotations and translations creates self-aligning exoskeleton joints. This lowers potentially painful interaction forces and reduces setup times. The primary disadvantages are the increased complexity and the reduction in interaction stiffness. The decoupling is found to be an essential advantage for the shoulder joint and is useful for the elbow joint. The DP is the preferred linkage mechanism. However, only further clinical practice and investigations will prove if decoupling is actually superior over conventional designs.

The decoupling principle is used in two exoskeletons: the passive Dampace, for force coordination training, and the upcoming hydraulically powered Limpact, for assist-as-needed training and quantifying movement disorders. So far, the initial reactions from therapists, patients, and scientists have been almost exclusively positive.

## REFERENCES

- [1] J. van der Lee, I. Snels, H. Beckerman, G. Lankhorst, R. Wagenaar, and L. Bouter, "Exercise therapy for arm function in stroke patients: A systematic review of randomized controlled trials," *Clin. Rehabil.*, vol. 15, no. 1, pp. 20–31, 2001.
- [2] T. Platz, "Evidence-based arm rehabilitation—A systematic review of the literature," *Nervenarzt*, vol. 74, no. 10, pp. 841–849, 2003.
- [3] G. Prange, M. Jannink, C. Groothuis-Oudshoorn, H. Hermens, and M. IJzerman, "Systematic review of the effect of robot-aided therapy on recovery of the hemiparetic arm after stroke," *J. Rehabil. Res. Dev.*, vol. 43, no. 2, pp. 171–184, 2006.
- [4] G. Kwakkel, B. Kollen, and H. Krebs, "Effects of robot-assisted therapy on upper limb recovery after stroke: A systematic review," *Neurorehabil. Neural Repair*, vol. 22, no. 2, pp. 111–121, 2008.
- [5] N. Hogan, H. Krebs, J. Charnarong, and P. Srikrishna, A. Sharon, "MIT-MANUS: A workstation for manual therapy and training. I," in *Proc. 2nd ROMAN*, Tokyo, Japan, Sep. 1–3, 1992, pp. 161–65.
- [6] T. Sukal, M. Ellis, and J. Dewald, "Shoulder abduction-induced reductions in reaching work area following hemiparetic stroke: Neuroscientific implications," *Exp. Brain Res.*, vol. 183, no. 2, pp. 215–223, 2007.
- [7] A. Nakai, T. Ohashi, and H. Hashimoto, "7 DOF arm type haptic interface for teleoperation and virtual reality systems," in *Proc. IROS*, Victoria, BC, Canada, Oct. 13–17, 1998, vol. 2, pp. 1266–1271.
- [8] R. Sanchez, E. Wolbrecht, R. Smith, J. Liu, S. Rao, S. Cramer, T. Rahman, J. Bobrow, and D. Reinkensmeyer, "A pneumatic robot for re-training arm movement after stroke: Rationale and mechanical design," in *Proc 9th ICORR*, E. Wolbrecht, Ed. Chicago, IL, Jun. 28–Jul. 1, 2005, pp. 500–504.
- [9] A. Frisoli, F. Rocchi, S. Marcheschi, A. Dettori, F. Salsedo, and M. Bergamasco, "A new force-feedback arm exoskeleton for haptic interaction in virtual environments," in *Proc 1st WHC*, Pisa, Italy, Mar. 18–20, 2005, pp. 195–201.
- [10] T. Nef, M. Mihelj, and R. Riener, "ARMin: A robot for patient-cooperative arm therapy," *Med. Biol. Eng. Comput.*, vol. 45, no. 9, pp. 887–900, 2007.
- [11] C. Carignan, J. Tang, S. Roderick, and M. Naylor, "A configuration-space approach to controlling a rehabilitation arm exoskeleton," presented at the 10th ICORR, Noordwijk, The Netherlands, Jun. 13–15, 2007.
- [12] J. Perry, J. Rosen, and S. Burns, "Upper-limb powered exoskeleton design," *IEEE-ASME Trans. Mech.*, vol. 12, no. 4, pp. 408–417, Aug. 2007.
- [13] D. Mayhew, B. Bachrach, W. Rymer, and R. Beer, "Development of the MACARM—A novel cable robot for upper limb neurorehabilitation," in *Proc. 9th ICORR*, Chicago, IL, Jun. 28–Jul. 1, 2005, pp. 299–302.
- [14] A. Stienen, E. Hekman, F. van der Helm, G. Prange, M. Jannink, A. Aalsma, and H. van der Kooij, "Freebal: Dedicated gravity compensation for the upper extremities," presented at the 10th ICORR, Noordwijk, The Netherlands, Jun. 13–15, 2007.
- [15] A. Schiele and F. van der Helm, "Kinematic design to improve ergonomics in human machine interaction," *IEEE Trans. Neural Syst. Rehabil. Eng.*, vol. 14, no. 4, pp. 456–469, Dec. 2006.
- [16] D. Romilly, C. Anglin, R. Gosine, C. Hershler, and S. Raschke, "A functional task analysis and motion simulation for the development of a powered upper-limb orthosis," *IEEE Trans. Rehabil. Eng.*, vol. 2, no. 3, pp. 119–129, Sep. 1994.
- [17] D. G. Caldwell, C. Favede, and N. Tsagarakis, "Dextrous exploration of a virtual world for improved prototyping," in *Proc. IEEE Int. Conf. Robot. Autom.*, May 16–20, 1998, vol. 1, pp. 298–303.
- [18] G. Wu, F. van der Helm, H. Veeger, M. Makhsous, P. Van Roy, C. Anglin, J. Nagels, A. Karduna, K. McQuade, X. Wang, F. Werner, and B. Buchholz, "ISB recommendation on definitions of joint coordinate systems of various joints for the reporting of human joint motion—Part II: Shoulder, elbow, wrist and hand," *J. Biomech.*, vol. 38, no. 5, pp. 981–992, 2005.
- [19] J. Lenarcic and M. Stanisic, "A humanoid shoulder complex and the humeral pointing kinematics," *IEEE Trans. Robot. Autom.*, vol. 19, no. 3, pp. 499–506, Jun. 2003.
- [20] G. Colombo, M. Joerg, R. Schreier, and V. Dietz, "Treadmill training of paraplegic patients using a robotic orthosis," *J. Rehabil. Res. Dev.*, vol. 37, no. 6, pp. 693–700, 2000.
- [21] R. Sanchez, J. Liu, S. Rao, P. Shah, R. Smith, T. Rahman, S. Cramer, J. Bobrow, and D. Reinkensmeyer, "Automating arm movement training following severe stroke: Functional exercises with quantitative feedback in a gravity-reduced environment," *IEEE Trans. Neural Syst. Rehabil. Eng.*, vol. 14, no. 3, pp. 378–389, Sep. 2006.
- [22] M. Bottlang, S. M. Madey, C. M. Steyers, J. L. Marsh, and T. D. Brown, "Assessment of elbow joint kinematics in passive motion by electromagnetic motion tracking," *J. Orthop. Res.*, vol. 18, no. 2, pp. 195–202, Mar. 2000.
- [23] A. Ericson, A. Arndt, A. Stark, P. Wretenberg, and A. Lundberg, "Variation in the position and orientation of the elbow flexion axis," *J. Bone Joint Surg. Br.*, vol. 85, no. 4, pp. 538–544, May 2003.
- [24] R. Clavel, "Delta, a fast robot with parallel geometry," in *Proc 18th ISIR*, Sydney, Australia, Nov. 6–10, 1988, pp. 91–100.
- [25] S. Grange, F. Conti, P. Rouiller, P. Helmer, and C. Baur, "The Delta haptic device," presented at the 5th Mechatron., Besancon, France, Jul. 7, 2001.
- [26] J. Herder, "Energy-free systems: Theory, conception and design of statically balanced spring mechanisms," Ph.D. dissertation, Delft Univ. Technol., Delft, The Netherlands, 2001.
- [27] A. Stienen, E. Hekman, F. van der Helm, G. Prange, M. Jannink, A. Aalsma, and H. van der Kooij, "Dampace: Dynamic force-coordination trainer for the upper extremities," presented at the 10th ICORR, Noordwijk, The Netherlands, Jun. 13–15, 2007.
- [28] J. Jonker and J. Meijaard, "SPACAR—computer program for dynamic analysis of flexible spatial mechanisms and manipulators," in *Multibody Systems Handbook*, W. Schiehlen, Ed. Berlin, Germany: Springer-Verlag, 1990, pp. 123–143.
- [29] G. Johnson, D. Carus, G. Parrini, S. Marchese, and R. Valsecchi, "The design of a five-degree-of-freedom powered orthosis for the upper limb," *PI Mech. Eng. H*, vol. 215, no. H5, pp. 275–284, 2001.
- [30] A. Stienen, E. Hekman, A. Schouten, F. Van der Helm, and H. Van der Kooij, "Suitability of hydraulic disk brakes for passive actuation of upper-extremity rehabilitation exoskeletons," *Appl. Bionics Biomech.*, to be published.
- [31] A. Stienen, E. Hekman, H. ter Braak, A. Aalsma, F. van der Helm, and H. van der Kooij, "Rotational hydro elastic actuator for a torque driven exoskeleton for the upper-extremities," presented at the Biorob, Scottsdale, AZ, Oct. 19–22, 2008.
- [32] A. Stienen, E. Hekman, H. Ter Braak, A. Aalsma, F. Van der Helm, and H. Van der Kooij, "Design of a rotational hydro-elastic actuator for an active upper-extremity rehabilitation exoskeleton," *IEEE Trans. Bio-Med. Eng.*, to be published.
- [33] A. Schiele, "An explicit model to predict and interpret constraint force creation in pHRI with exoskeletons," in *Proc ICRA*, 2008, pp. 1324–1330.